Journal of
Ceramic Science
and Technology

J. Ceram. Sci. Tech., **01** [01] 33-40 (2010)
DOI: 10.4416/JCST2010-00008
available online at: http://www.ceramic-science.com

A New Bioactive Glass Composition for Bioceramic Scaffolds

Devis Bellucci*, Valeria Cannillo and Antonella Sola

Dipartimento di Ingegneria dei Materiali e dell'Ambiente, Università degli Studi di Modena e Reggio Emilia, Via Vignolese 905, 41100 Modena, Italy

received April 07, 2010; received in revised form May 21, 2010; accepted July 15, 2010

Abstract

Bioactive-glass-derived scaffolds are crucial in bone tissue engineering since they act as temporary templates for tissue regrowth, providing structural support to the cells in a resulting 3D architecture. However, many issues remain open with regard to their design. On the one hand, bioceramic scaffolds should be bioactive, highly porous and should possess adequate mechanical properties; on the other hand, attempts to improve the mechanical properties of the widely used 45S5 Bioglass® turn the bioactive glass itself into a glass-ceramic, with non-trivial effects on the resulting scaffold bioactivity. In this work, for the first time a new bioactive glass composition was employed to produce scaffolds for bone tissue engineering. The new glass composition can be treated at a relatively low temperature and it is characterized by a reduced tendency to crystallize compared to the 45S5 Bioglass®. Moreover, the presented scaffolds are realized with a recently developed technique described here in detail. The resulting samples are highly porous and bioactive. Additionally, they possess a resistant and at the same time permeable surface similar to a shell, which ensures good manageability.

Keywords: bioceramics, porous materials, scaffolds, glass-ceramics.

I. Introduction

In the last few years, bioactive glasses have shown themselves to be some of the most promising materials for bone tissue regeneration and repair[1, 2]. Many bioactive glasses are based on the SiO_2-CaO-Na_2O-P_2O_5 system[3]. Of these, the 45S5 Bioglass®[4, 5], the proportions of which are 45 wt. % SiO_2, 24.5 wt. % CaO, 24.5 wt. % Na_2O and 6 wt. % P_2O_5, is the most bioactive glass, being able to bond to both soft and hard tissues. This glass composition, originally determined by Hench and colleagues at the end of the 1960s, was selected to provide a large amount of CaO with some P_2O_5 in a Na_2O-SiO_2 matrix. In the same compositional system, silica percentages higher than 60 wt. % make glasses substantially bio-inert, while SiO_2 contents between 52 and 60 wt. % result in a slow bonding rate. Moreover, it was observed that glasses with larger percentages of P_2O_5 do not bond to bone[6].

Since the pioneering studies on 45S5 Bioglass® by Hench and colleagues[7], many bioactive glass compositions have been developed[8 – 10]. Presently, one of the main objectives of research in this field is to investigate the effect of a crystallization process on the glass' degree of bioactivity, i.e. on its ability to form a superficial hydroxyapatite (HA) layer when soaked in a simulated body fluid solution (SBF), which can be evaluated by means of *in vitro* tests[11]. The *in vitro* HA formation, in fact, is considered a necessary requirement for adequate implant biointegration.

The major problem limiting the use of bioactive glasses as load-bearing implants is their brittleness, therefore appropriate treatment, such as sintering, are necessary to enhance their mechanical properties. Unfortunately, conventional sintering processes usually require high-temperature cycles, which are likely to promote glass crystallization[12, 13]. For this reason, the mechanisms that turn bioactive glasses into glass-ceramics as a result of thermal treatment and the degree of bioactivity of partially crystallized systems are crucial topics. These topics become even more crucial when bioactive glasses are employed for the realization of scaffolds in bone tissue engineering. Scaffolds are artificial structures designed as temporary templates for cell adhesion and proliferation[13, 14]. In a typical tissue engineering step, they provide mechanical support to the growing bone tissue and they are progressively resorbed with a degradation rate that matches the growth rate of the new tissue. In order to serve as bone grafts, scaffolds should be highly biocompatible and bioactive and they should optimally mimic the structure of bone tissue. First of all, they should be highly porous, with a porosity of at least 50-60 vol. %, although higher porosity values, i.e. up to 90 vol. %, would be desirable[15, 16]. Moreover they should present an interconnected porosity, with pore sizes in the range of hundreds of microns (100-500 μm) to allow cell penetration and vascularization[17, 18]. To conclude, they should exhibit adequate mechanical properties and they should possess a permeable and, at the same time, resistant surface, which is necessary for them to be handled without any damage for *in vitro* tests and *in vivo* applications.

In order to fabricate reliable scaffolds, with sufficient mechanical properties, proper thermal treatments are required to consolidate their structure. However, as previ-

* Corresponding author: devis.bellucci@unimore.it

ously mentioned, 45S5 Bioglass®-based bioceramic scaffolds are usually sintered at temperatures that induce a complete crystallization of the glass, which may affect the bioactivity. In fact, although 45S5 Bioglass®-derived glass-ceramics typically remain bioactive, the corresponding HA rate formation *in vitro* is reduced by crystallization; in particular, the rate of HA formation decreases when the percentage of crystallization increases[3, 19]. In order to overcome this hurdle, new glass compositions with a reduced tendency to crystallize are expected to open interesting scenarios for scaffold applications.

Recently, a new glass composition, named BioK and inspired by the 45S5 Bioglass®, was formulated by substituting the sodium oxide with potassium oxide[20]. The potassium oxide is expected to reduce the tendency to crystallize of the parent glass. In this work, for the first time the BioK is applied for the realization of bioceramic scaffolds. The scaffolds themselves are fabricated with an emergent technique, which has been briefly discussed in a previous short communication regarding 45S5 Bioglass®[21]. The novel samples, named "shell scaffolds", are obtained by means of a modified replication technique. The standard and widely used replication method[13], which involves the production of ceramic foams by coating a polymeric sponge, can lead to scaffolds with poor mechanical properties and brittle surfaces. Instead, the new scaffolds combine a high porosity and good manageability, which are derived from their external surface resembling a resistant but very porous shell. In the work described here, the BioK glass was chosen instead of the well-established 45S5 Bioglass® because the BioK shell scaffolds can be sintered at a lower temperature. This offers various advantages. First of all, the peculiar thermal behaviour of the BioK glass helps preserve the amorphous nature of the scaffolds; moreover thermal treatment at lower temperatures results in a cheaper technological protocol. Even though the main focus of the paper was on the new glass, 45S5 Bioglass® shell scaffolds were also realized and used as reference samples, especially for the *in vitro* characterization. In fact, particular emphasis was given to the behaviour of the realized scaffolds in a SBF solution, which is indicative of their bioactivity.

II. Materials and Methods

(1) Scaffold fabrication

The BioK composition was derived from that of the 45S5 Bioglass®, but the sodium oxide was substituted with potassium oxide. Hence, the resulting BioK proportions were 46.1 mol% SiO_2, 26.9 mol% CaO, 24.4 mol% K_2O (as a substitute for the Na_2O) and 2.6 mol% P_2O_5[20]. A basic characterization of the glass has been reported elsewhere[20], however, an additional study of the BioK thermal behaviour was conducted by means of heating microscope analysis (Expert System Solutions, Misura ODHT HSM 1600-80). The glass samples (powders) were heated from room temperature to 1200 °C at 10 °C/min. The main objective of the test was to define the sintering temperature of the BioK, in order to optimize the thermal treatment of the scaffolds.

In order to produce the scaffolds, the BioK was prepared by melting appropriate raw materials in powder form (commercial reagent grade SiO_2, $CaCO_3$, K_2CO_3 and $K_3PO_4{\cdot}H_2O$ supplied by Carlo Erba Reagenti, Italy) in a platinum crucible at 1450 °C for 1 h and then by rapidly quenching the melt in water. The obtained frit was then ball-milled and sieved to a final grain size below 60 mm. The grain size distribution was measured with a laser granulometer (Mastersizer 2000, Malvern Instruments, UK) and is shown in fig. 1. The same procedure was also applied to prepare the 45S5 Bioglass®; the corresponding raw powder materials were commercial SiO_2, $CaCO_3$, $Na_3PO_4{\cdot}12H_2O$ and Na_2CO_3 (Carlo Erba Reagenti, Italy).

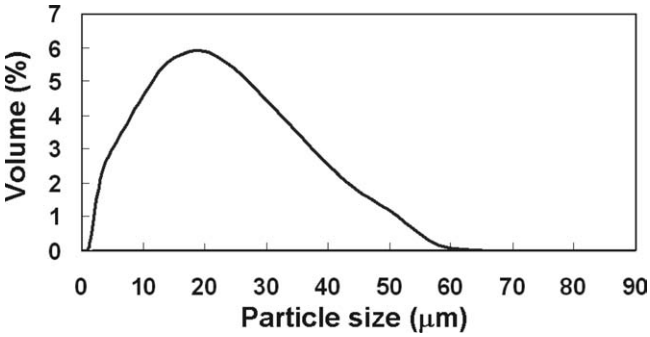

Fig. 1: Particle size distribution of the BioK powders (starting material).

Both the BioK and the 45S5 Bioglass® were used to produce the scaffolds in accordance with the new protocol, which is based on a modified replication technique[13, 22]. In accordance with the replication method, a polyurethane sponge was used as an organic template for the scaffolds. Firstly, a glass slurry was obtained by dispersing the glass powder, i.e. BioK or 45S5 Bioglass®, into distilled water together with a polyvinylic binder (Henkel Italia S.p.A., Milan – Italy). The polyvinylic binder was used to control the slurry viscosity and to promote the adhesion of the glass particles to the sponge during immersion. The selected weight ratio of the slurry components was: 59 % water, 29 % BioK (or 45S5 Bioglass®) and 12 % polyvinylic binder. The procedure was performed under magnetic stirring. The polyurethane sponges were immersed in the slurry and then retrieved from the suspension; however, unlike in the traditional replication technique, they were not squeezed but kept fully loaded with the slurry. Subsequently, the samples were dried under a multidirectional vigorous air flux at 100 °C for 15 minutes. Meanwhile, the samples were maintained in rotation in the air flux to keep them slurry-loaded and to ensure an even distribution of the slurry within the samples themselves. At the end of the drying process, the samples, referred to as green bodies, were coated with an external thin layer made of glass particles and binder. Finally, the glass (BioK or 45S5 Bioglass®) green bodies were introduced into a furnace at room temperature and heat-treated at a proper sintering temperature for three hours, with the aim of burning out the organic phase and consolidating the glass structure. The heating rate was 5 °C/min up until 400 °C and subsequently 10 °C/min. As previously mentioned, the sintering process of the BioK required lower temperatures than for the 45S5 Bioglass®. The former, in fact, was sintered at 750 °C, while

the latter was heat-treated at 1050 °C (preliminary tests proved that the 45S5 Bioglass® scaffolds treated at 750 °C were not fully sintered with the processing schedule proposed in the present research).

(2) Characterization and assessment of bioactivity in simulated body fluid

The microstructure of BioK and the 45S5 Bioglass® scaffolds was investigated with a scanning electron microscope, SEM (ESEM Quanta 2000, FEI Co., Eindhoven, Netherlands), before and after *in vitro* tests. The instrument was operated in low-vacuum mode, with a pressure of 0.5 Torr. The chemical analyses were performed by means of X-ray Energy Dispersion Spectroscopy, EDS (Inca, Oxford Instruments, UK), in order to observe the HA formation.

The total porosity $P_{\%}$ (vol. %) of the scaffolds was evaluated by measuring the weight of cubic samples; $P_{\%}$ can be easily calculated by means of the following equation

$$P_{\%} = \left(1 - \frac{W_f}{W_0}\right) \times 100$$

where W_f is the measured weight of the scaffold and W_0 is the theoretical weight, obtained by multiplying the scaffold volume by the corresponding glass density, i.e. ρ = 2.7 g/cm^3 for 45S5 Bioglass®[23] and ρ = 2.5 g/cm^3 for BioK. The BioK density was measured by means of a pycnometer test (Micromeritics AccuPyc 1330, Georgia, USA).

X-ray diffraction (XRD) analyses were performed in order to investigate the crystallinity of the scaffolds, as produced and after *in vitro* tests. The samples were first ground into a powder and then analyzed with a PANalytical X'pert PRO diffractometer employing Cu kα radiation. Data were collected in the 2θ angular range 10-70°, with steps of 0.02° and 5 s/step.

According to the standard *in vitro* protocol developed by Kokubo and colleagues[11], the bioactivity of the obtained scaffolds was tested *in vitro* by soaking them in a simulated body fluid solution (SBF), i.e. an acellular solution with inorganic ion concentrations similar to those of the human extracellular fluid. With this aim, the samples were immersed in flasks containing 20 ml SBF. The flasks were kept at a controlled temperature of 37 °C and the SBF solution was refreshed every 48 hours. The samples were extracted from the SBF after set times of 3, 7 and 14 days. Once extracted from the solution, the samples were left to dry at ambient temperature.

III. Results and Discussion

The results of the heating microscope analysis of the BioK powder are shown in fig. 2. Taking these findings into account, the green bodies were treated at 750 °C for three hours in order to consolidate them. Since the polyurethane sponge was completely removed at 500 °C, no contamination of the scaffolds was observed after the thermal treatment. It should be noted that the temperature chosen for the BioK scaffold production was rather lower than that used for the 45S5 Bioglass® samples, which were treated at 1050 °C. In fact, as already mentioned, preliminary tests proved that the 45S5 Bioglass® scaffolds treated at 750 °C were not fully sintered. Even if the present contribution proposed a new protocol to produce the scaffolds (a modified replication technique), this result is in a good agreement with the densification behaviour of 45S5 Bioglass®-derived scaffolds described in the literature[13, 24].

Fig. 3 shows the morphology of the polymeric sponge employed as a template for the scaffold preparation. It is possible to observe its highly interconnected pore structure resembling cancellous bone. In particular, the pore size varies between 100 µm and 1000 µm, while the thickness of the struts separating the pores measures a few tens of microns. Since the polymeric sponge can be cut into different shapes, the proposed fabrication protocol is very versatile.

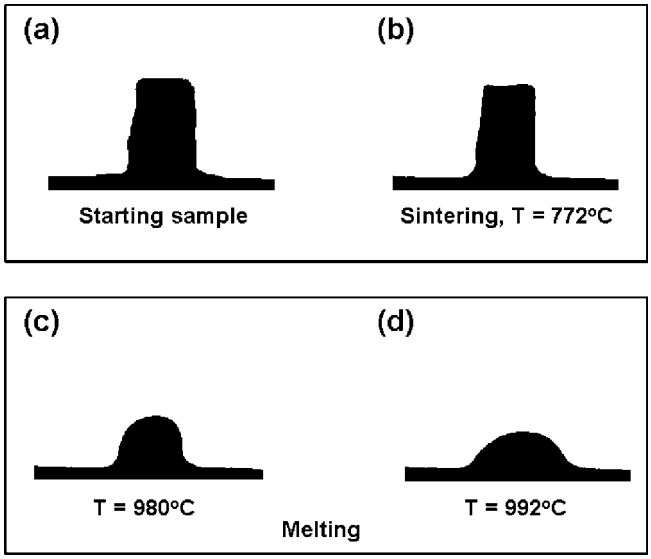

Fig. 2: Heating microscope analysis of the BioK powders: starting specimen (a), sintering temperature (b), half-sphere (c) and melting (d) temperatures.

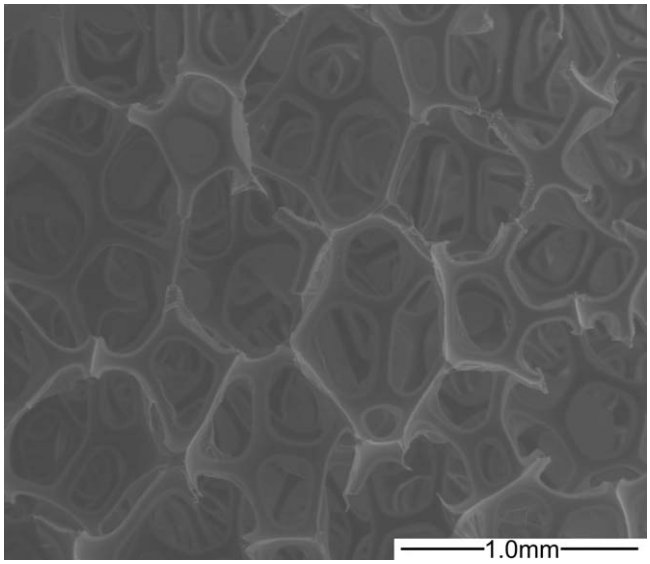

Fig. 3: Micrograph of the polymeric sponge employed to realize shell scaffolds (SEM).

Various BioK scaffolds are presented in fig. 4. Since the architecture is almost the same for both the BioK and 45S5 Bioglass® samples, only the former are presented in detail.

The external surface of the scaffolds reveals an original structure characterized by a "grid-like" morphology, with

large pores and thick trabecolae between them. This structure is similar to a porous shell and, for this reason, the samples are referred to as "shell scaffolds". The outer shell makes it easy to handle the samples without any damage, because it behaves like an esoskeleton for the entire scaffold, and this is one of the main advantages of the new shell scaffolds. Additionally, their external surface guarantees excellent permeability[21]. For these reasons, the developed technique exceeds the limits of the conventional replication method, which produces brittle scaffolds that are very difficult to handle.

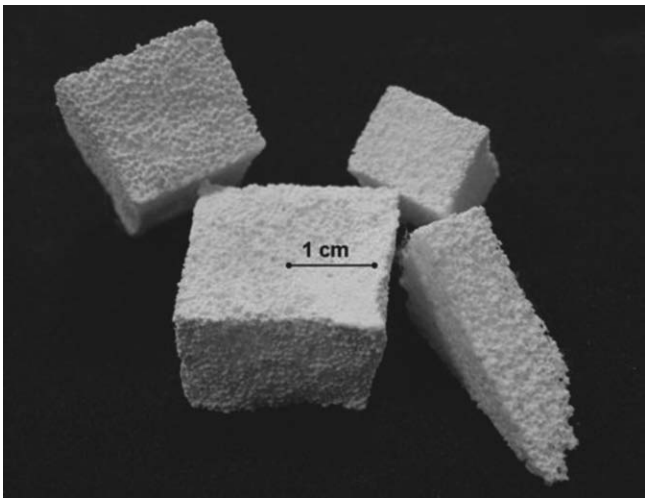

Fig. 4: Digital camera image of BioK shell scaffolds with different shapes.

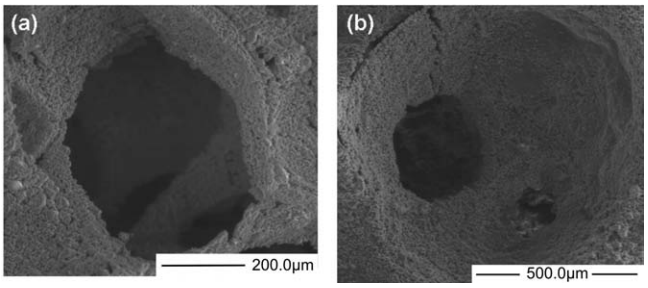

Fig. 5: Micrographs showing the microstructure of the BioK shell scaffolds: detail of the scaffold surface (SEM).

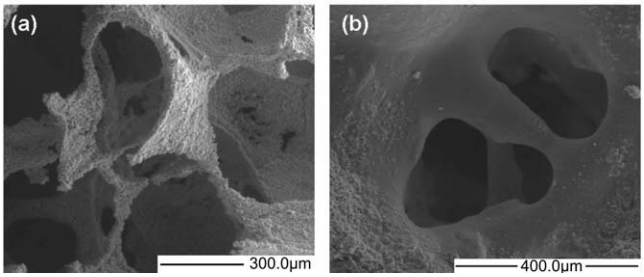

Fig. 6: Micrographs showing the microstructure the BioK shell scaffolds: detail of the internal structure (SEM).

The microstructural analysis presented in fig. 5 clearly shows the excellent connection between the outer shell and the inner part of the samples. The micrographs of the internal microstructure shown in fig. 6, on the other hand, reveal the presence of an open and interconnected pore network, resembling the parent sponge structure (fig. 3). Pores larger than 100 µm are abundantly present and therefore the structure completely satisfies the requirements to ensure bone tissue ingrowth[15, 16, 25]. Moreover, macropores over 100 µm are fundamental for good vascularization of the implant and to allow the macrophages to enter the graft in case of bacterial infections[26]. At the same time, the realized samples are characterized by a bimodal pore network since not only macropores, but also micropores (size below 100 µm) are present. In fact, the decomposition gases generated by the evaporation of the organic sponge caused the development of a rich microporosity. An adequate microporosity, which creates a roughness on the scaffold walls, is a key factor to promote diffusion of fluids and to foster proteins and cells adhesion *in vivo*[27, 28]. Fig. 6(b) suggests that an optimal degree of sintering of the struts was achieved: the trabeculae, indeed, are so densified that it is no longer possible to distinguish the starting glass particles.

The average porosity, resulting from density measurements, is about 80 vol. % for both BioK and 45S5 Bioglass® samples. This value satisfies the requirements to promote effective bone ingrowth *in vivo*[25]. In addition, it should be noted that, in this kind of scaffold, most of the glass is concentrated in the external shell and therefore the internal porosity is expected to be higher than the calculated (mean) value.

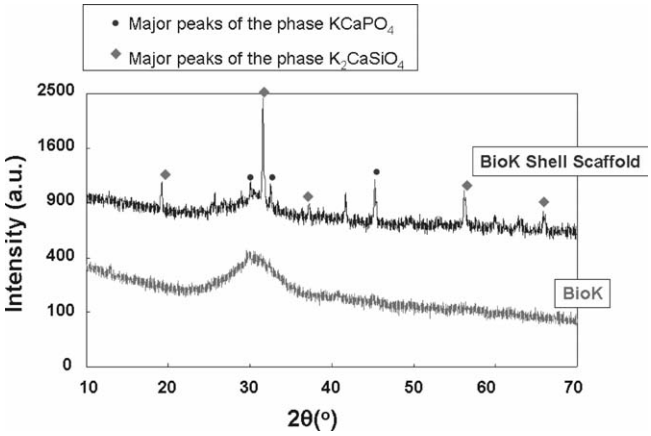

Fig. 7: XRD spectra of the unsintered BioK powder and of the BioK Shell scaffold.

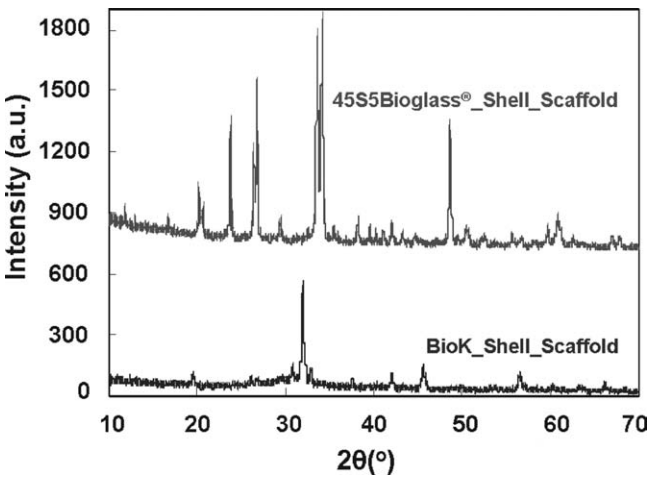

Fig. 8: XRD spectra of BioK- and 45S5 Bioglass®-derived shell scaffolds.

The XRD analysis performed on the BioK starting powder and on a BioK shell scaffold ground into a powder is shown in fig. 7. The pattern of the BioK powder was characterized by a broad halo, indicating that the starting glass was completely amorphous. It is worth noting that, after the thermal treatment, although some peaks appeared in the XRD pattern (corresponding to the $KCaPO_4$ and K_2CaSiO_4 crystalline phases), the broad halo was still present. This fact indicates the presence of a significant amount of amorphous phase even after the thermal treatment, confirming the limited crystallization tendency of the BioK. This looks very promising with regard to retaining the material's bioactivity. Analogous behaviour cannot be observed in the 45S5 Bioglass®-derived scaffolds, the XRD pattern of which is compared to that of the BioK in fig. 8. The Bioglass®-derived scaffolds, in fact, were characterized by an almost complete crystallization of the starting glass[13], with an extensive development of $Na_2CaSi_2O_6$, a crystalline phase frequently reported in literature studies on the thermal behaviour of the 45S5 Bioglass®[29, 30].

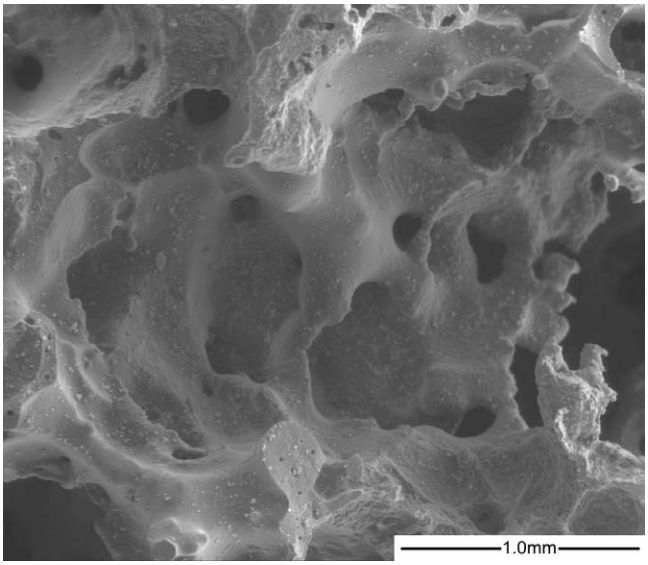

Fig. 9: Micrograph showing the internal structure of the BioK shell scaffold after immersion in simulated body fluid for 3 days (SEM).

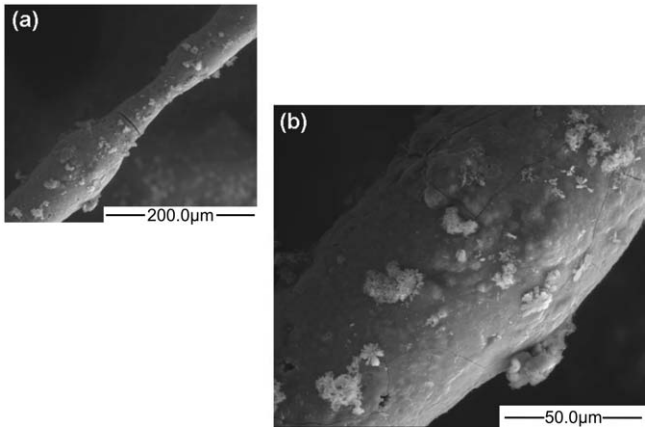

Fig. 10: Micrograph showing the internal structure of the BioK shell scaffold after immersion in simulated body fluid for 3 days (SEM).

Figs. 9 and 10 show representative micrographs of the surface of the BioK shell scaffolds after soaking in SBF for three days. Some HA globular agglomerates can be seen on the scaffold surface, which is uniformly covered by a silica gel layer. This fact is even more evident in fig. 10, which reports the detail of a dense trabecula on which the white agglomerates of the precipitated HA can be observed. Since the development of HA on bioactive materials is conditioned by the presence of OH^- groups on their surface[31, 32], it may be suggested that the distribution of the first HA agglomerates follows the location of OH^- groups on the trabeculae, which may be influenced by the local crystallization revealed by XRD analysis.

The EDS analysis performed on the whole area shown in fig. 11 revealed the presence of Ca and P in proportions similar to that in HA, since the Ca/P ratio is about 1.9, while in the stoichiometric HA it is 1.67[33]. The presence of Si is due to the gel-like layer rich in silica underneath the HA crystals. In fact, according to the model originally proposed by Hench and colleagues[34, 35], the ability of a bioactive glass to build tenacious bonds with the surrounding bone is attributed to a complex sequence of reactions; in particular, the bioactive glass starts its dissolution by exchanging alkali or alkaline-earth cations, such as K^+ in the BioK case, with H^+ or H_3O^+ ions from the physiological media. During this step the interfacial pH increases. The high specific surface area, which is typical of macroporous scaffolds, may influence the kinetics of

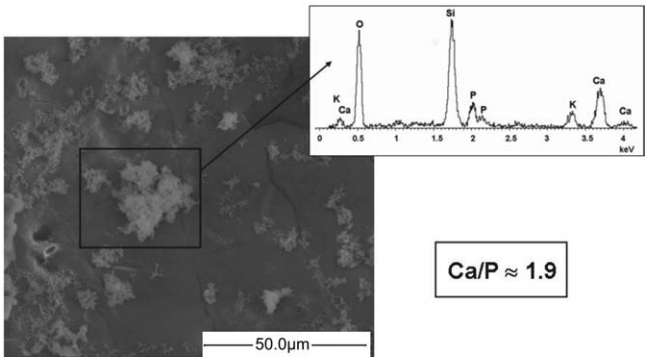

Fig. 11: Hydroxyapatite formed on the surface of BioK shell scaffolds after immersion in simulated body fluid for 3 days: details and EDS results of the analysis conducted on the whole area indicated (SEM).

bioactivity mechanisms. Here, in fact, a fast ion exchange with SBF may be observed and the pH value of the solution rapidly increases. Subsequently, silanol groups (Si-OH) form at the glass/solution interface. Rearrangement and polycondensation of neighbouring silanol groups results in a silica gel layer on the glass surface. The cracks in the silica gel visible in fig. 11 are caused by the drying of the gel layer itself, which originally is highly hydrated.

After longer immersion periods in simulated body fluid, an increase in the amount of precipitated HA on the scaffold surface was observed. The surface texture reported in fig. 12 shows that the HA globular precipitates cover the silica gel layer entirely after 7 days soaking in SBF. In particular, the HA precipitate also covers the internal pore surface. Some considerations may be made taking into account the EDS analysis presented in fig. 13. Firstly, as previously mentioned, the potassium content of the BioK surface is lower compared to the spectra in fig. 11, owing

to ion leaching, and it approaches zero, therefore the scaffold surface is almost depleted in K^+. The ratio between Ca and P in this case is about 1.67, similar to that in stoichiometric HA. Finally, although Si is still present as a result of the silica gel, its content appears lower in amount because of the thicker HA layer above it. The EDS analysis of the samples after 14 days in SBF is very similar to the 7-day analysis, therefore it is not described. However, in this case the scaffold surface is completely covered by HA, many struts have completed their dissolution and, locally, it is difficult to identify the starting spongy-like structure of the shell scaffold. On the basis of these good results, *in vivo* bioactivity of the shell scaffold can also be expected, as well as adequate vascularization of the scaffold itself.

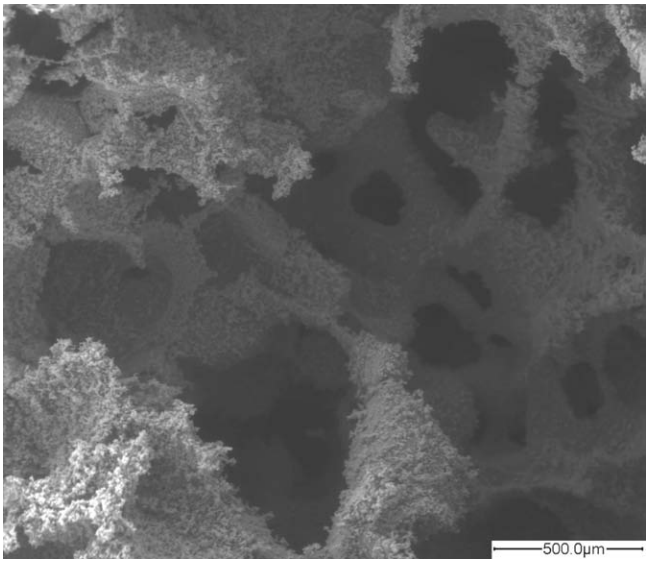

Fig. 12: Hydroxyapatite formed on the surface of BioK shell scaffolds after immersion in simulated body fluid for 7 days (SEM).

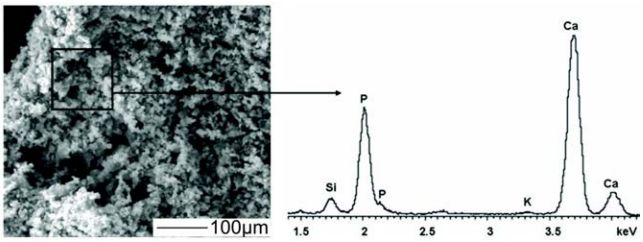

Fig. 13: Hydroxyapatite formed on the surface of BioK shell scaffolds after immersion in simulated body fluid for 7 days: detail and EDS result of the analysis conducted on the area indicated (SEM).

The diffraction pattern obtained for the BioK scaffolds after milling is reported in fig. 14 for 3, 7 and 14 days immersion in SBF. As mentioned above, the thermal treatment performed to produce the scaffolds induced the nucleation of two main crystalline phases, which were identified as $KCaPO_4$ and K_2CaSiO_4. On the other hand, the permanence of the broad halo due to the reduced tendency to crystallize of BioK should also be noted. Analysing the XRD spectra of the immersed samples, it is possible to observe the dissolution of the crystalline phases with increasing soaking time. In particular, several peaks of the K_2CaSiO_4 phase disappear after 14 days of soaking in SBF. Even if the presence of HA on the immersed scaffolds was proved by ESEM investigation and EDS analysis, it was not possible to identify the peaks of HA in the XRD spectra. Unfortunately, in fact, the peaks of the crystalline phases present in the BioK scaffolds and the peaks of HA overlap.

In order to assess the *in vitro* behaviour of the BioK scaffolds, a parallel study with 45S5 Bioglass® samples was conducted. A direct comparison between the HA formed on the surface of 45S5 Bioglass®- and BioK-derived shell scaffolds after immersion in SBF is shown in fig. 15. Although it is difficult to measure – and therefore to compare – from a quantitative point of view the bioactivity of the samples by means of *in vitro* tests, some conclusions are possible. HA uniformly covers the BioK samples' surface (Fig. 15(b)) already after one week in SBF. In particular, it is difficult to discern the silica-gel layer underneath the HA, both inside and outside the pores. On the contrary, although a large amount of HA agglomerates can be observed on the 45S5 Bioglass® samples, they do not cover them uniformly. Since the scaffold microstructure and porosity are almost the same for BioK and 45S5 Bioglass®

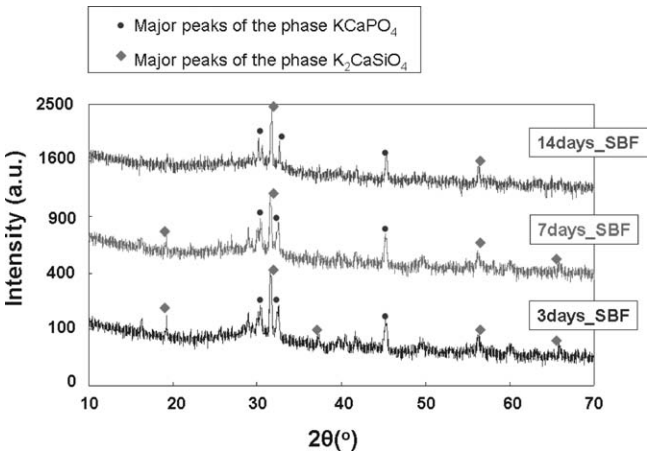

Fig. 14: XRD spectra of BioK Shell scaffold after immersion in simulated body fluid for 3, 7 and 14 days.

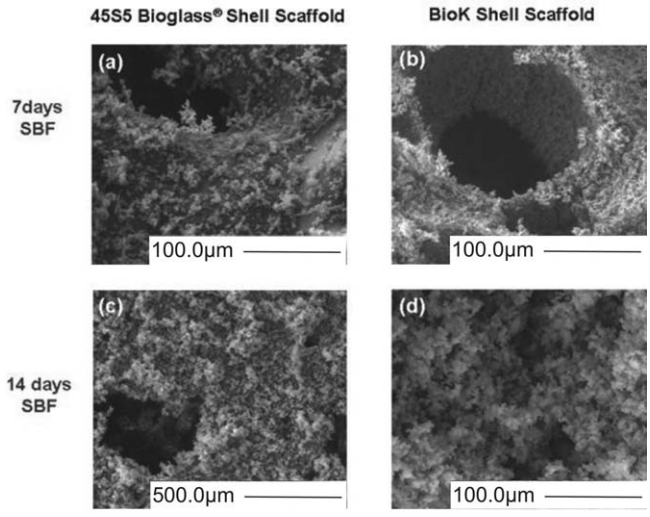

Fig. 15: Hydroxyapatite formed on the surface of 45S5 Bioglass®-derived (a, c) and BioK (b, d) shell scaffolds (a, c) after immersion in simulated body fluid for 7 and 14 days (SEM).

samples, their different *in vitro* behaviour can be attributed to their different degree of crystallization. In addition,

the different *in vitro* solubility of the corresponding crystalline phases probably plays an important role in the HA precipitation. After 14 days in SBF (Fig. 15(c, d)), both samples are completely covered by a HA layer. However, the dissolution process in BioK samples seems to be more advanced, since it is difficult to identify the original pore network. For these reasons, the bioactivity of the BioK-derived scaffolds can be expected to be equal or even superior to that of the 45S5 Bioglass® scaffolds. Also taking into account the cheaper heat treatment required for BioK samples, this new bioactive glass appears a promising alternative as scaffolding material.

IV. Conclusions and Prospects

In this work, for the first time, an innovative protocol, recently developed to realize shell scaffolds for bone tissue engineering, was employed with BioK, i.e. a new glass composition, as starting glass. BioK was formulated by substituting the sodium oxide with potassium oxide in the typical 45S5 Bioglass® composition. Although the potassium oxide is expected to reduce the tendency to crystallize of the parent glass, this fact has not been exploited to produce scaffolds yet. The possibility of realizing scaffolds by means of bio-glasses that remain largely amorphous even after thermal treatment opens up promising scenarios. Moreover, the scaffolds presented in this work, produced with a modified replication technique, combine high porosity and manageability thanks to their shell-like external surface. For comparison, 45S5 Bioglass® shell scaffolds were also realized.

The XRD analysis performed on the BioK shell scaffolds confirmed the presence of a significant residual amorphous phase. This is due to the glass composition, which makes it possible to sinter the scaffolds at a relatively low temperature compared to that required for the 45S5 Bioglass®-based scaffolds. The shell scaffolds were tested *in vitro* by immersing them in a simulated body fluid in order to evaluate their bioactivity. The samples exhibited high bioactivity, in fact many HA agglomerates were observed on the sample surface already after three days in SBF. A comparison between results for the BioK and 45S5 Bioglass® scaffolds revealed that the former possessed a comparable (or even superior) degree of bioactivity.

Further studies on BioK-based shell scaffolds are in progress. Firstly, a mechanical characterization of the proposed samples would be necessary. Additionally, different slurry compositions are currently under evaluation. In particular, the possibility of adding further pore-generating agents, such as polyethylene powders, to the BioK slurry for sponge impregnation is being studied. The main objective, of course, is to increase the porosity of the final samples. Finally, it will be interesting to test *in vivo* BioK shell scaffolds in a biological reactor.

References

1 Ikada, Y., Tissue Engineering, Volume 8: Fundamentals and Applications, Academic Press (2006).

2 Salgado, A. J., Coutinho, O. P., Reis, R. L., Bone Tissue Engineering: State of the art and future trends, Macromol. Biosci. **4**, 743-765 (2004).

3 Peitl, O., Canotto, E. D., Hench, L. L., Highly bioactive P_2O_5-Na_2O-CaO-SiO_2 glass-ceramics, *J. Non-Crys. Solids* **292**, 115-126 (2001).

4 Hench, L. L., The story of Bioglass®, *J. Mater. Sci: Mater. Med.* **17**, 967-978 (2006).

5 Yamamuro, T., Hench, L. L., Wilson, J. (Eds.), Handbook on bioactive ceramics: bioactive glasses and glass-ceramics, Vol. I. CRC Press, Boca Raton, FL (1990).

6 Hench, L. L., Bioceramics, From Concept to Clinic, *J. Am. Ceram. Soc.* **74**(7), 1487-1510 (1991).

7 Hench, L.L., Splinter, R. J., Allen, W. C., Greenlee, T. K. , Bonding mechanisms at the interface of ceramic prosthetic materials, *J. Biomed. Mater. Res. Symp.* **2** (Part I): 117-141 (1971).

8 Elgayar, I., Aliev, A. E., Boccaccini , A. R., Hill, R. G., Structural analysis of bioactive glasses, *J. Non-Crys. Solids* **351**, 173-183 (2005).

9 Lockyer, M. W. G., Holland, D., Dupree, R., NMR investigation of the structure of some bioactive and related glasses, *J. Non-Crys. Solids* **188**, 207-219 (1995).

10 Brink, M., The influence of alkali and alkaline earths on the working range for bioactive glasses, *J. Biomed. Mater. Res.* **36**, 109-117 (1997)

11 Kokubo, T., Takadama, H., How useful is SBF in predicting *in vivo* bone bioactivity?, *Biomaterials* **27**, 2907-2915 (2006).

12 Boccaccini, A. R., Chen, Q. Z., Lefebvre, L., Gremillard, L., Chevalier, J., Sintering, crystallization and biodegradation behaviour of Bioglass®-derived glass-ceramics, Faraday Discuss. **136**, 27-44 (2007).

13 Chen, Q. Z., Thompson, I. D., Boccaccini, A. R., 45S5 Bioglass®-derived glass-ceramic scaffolds for bone tissue engineering, *Biomaterials* **27**, 2414-2425 (2006).

14 Rezwan, K., Chen, Q. Z., Blaker, J. J., Boccaccini, A. R., Biodegradable and bioactive porous polymer/inorganic composite scaffolds for bone tissue engineering, *Biomaterials* **27**, 3413-3431 (2006).

15 Karageorgiou, V., Kaplan, D., Porosity of 3D biomaterial scaffolds and osteogenesis, *Biomaterials* **26**, 5474-5491 (2005).

16 Salgado, A. J., Coutinho, O. P., Reis, R. L., Bone Tissue Engineering: State of the art and future trends, *Macromol. Biosci.* **4**, 743-765 (2004).

17 Mastrogiacomo, M., Scaglione, S., Martinetti, R., Dolcini, L., Beltrame, F., Cancedda, R., Quarto, R., Role of scaffold internal structure on in vivo bone formation in macroporous calcium phosphate bioceramics, *Biomaterials* **27**, 3230-3237 (2006).

18 Ochoa, I., Sanz-Herrera, J. A., Garcia-Aznar, J. M., Doblaré, M., Yunos, D. M., Boccaccini, A. R., Permeability evaluation of 45S5 Bioglass®-based scaffolds for bone tissue engineering, *J. of Biomechanics* **42**, 257-260 (2009).

19 Filho, O. P., LaTorre, G. P., Hench, L. L., Effect of crystallization on apatite-layer formation of bioactive glass 45S5, J. *Biomed. Mater. Res.* **30**, 509-514 (1996).

20 Cannillo, V., Sola, A., Potassium-based composition for a bioactive glass. *Ceram. Int.* **35**, 3389-3393 (2009).

21 Bellucci, D., Cannillo, V., Sola, A., Shell Scaffolds: a new approach towards high strength bioceramic scaffolds for bone regeneration, *Materials Letters* **64**, 203-206 (2010).

22 Vitale-Brovarone, C., Miola, M., Balagna, C., Verné, E., 3D-glass-ceramic scaffolds with antibacterial properties for bone grafting, *Chemical Engineering Journal* **137**, 129-136 (2008).

23 Lopez-Esteban, S., Saiz, E., Fujino, S., Oku, T., Suganuma, K., Tomsia, A. P., Bioactive glass coatings for orthopaedic metallic implants, *J. Eur. Cer. Soc.* **23**, 2921-2930 (2003).

24 Bretcanu, O., Samaille, C., Boccaccini, A. R., Simple methods to fabricate Bioglass®-derived glass-ceramic scaffolds exhibiting porosity gradient, *J. Mater. Sci.* **43**, 4127-4134 (2008).

25 Gautier, O., Bouler, J. M., Aguado, E., Pilet P., Daculsi, G., Macroporous biphasic calcium phosphate ceramics: influence

of macropore diameter and macroporosity percentage on bone ingrowth, *Biomaterials* **19**, 133-139 (1998).

26 De Aza, P. N., Luklinska, Z. B., Santos, C., Guitian, F., De Aza, S., *Biomaterials* **24**, 1437-1445 (2003).

27 Deligianni, D. D., Katsala, N. D., Koutsoukos P. G., Missirlis, Y. F., Effect of surface roughness of hydroxyapatite on human bone marrow cell adhesion, proliferation, differentiation and detachment strength, *Biomaterials* **22** (1), 87-96 (2001).

28 Schwarts, Z., Boyan, B. D., *J. Cell. Biochem.* **56**, 340-347 (1994).

29 Lefebvre, L., Gremillard, L., Chevalier, J., Zenati, R., Bernache-Assolant, D., Sintering behaviour of 45S5 bioactive glass, *Acta Biomaterialia* **4**, 1894-1903 (2008).

30 Lin, C. C., Huang, L. C., Shen, P., $Na_2CaSi_2O_6$-P_2O_5 based bioactive glasses. Part 1: Elasticity and structure, *J. Non-Crys. Solids* **351** (40-42), 3195-3203 (2005).

31 Kokubo, T., Apatite formation on surfaces of ceramics, metals and polymers in body environments, *Acta Mater.* **46** (7), 2519-2527 (1998).

32 Kokubo, T., Kim, H. M., Kawashita, M., Novel bioactive materials with different mechanical properties, *Biomaterials* **24**, 2161-2175 (2003).

33 Liu, H., Yazici, H., Ergun, C., Webster, T. J., Bermek, H., An in vitro evaluation of the Ca/P ratio for the cytocompatibility of nano-to-micron particulate calcium phosphates for bone regeneration, *Acta Biomaterialia* **4**, 1472-1479 (2008).

34 Hench, L. L., Paschall, H. A., Direct Chemical Bonding between Bio-Active Glass-Ceramic Materials and Bone, *J. Biomed. Mater. Res. Symp.*, **4**, 25-42 (1973).

35 Kim, C. Y., Clark, A. E., Hench, L. L., Early stages of calcium-phosphate layer formation in bioglasses, *J. Non-Crys. Solids* **113**, 195-202 (1989).